

Role of Death Receptors-associated Lipid Rafts in Oxaliplatin-induced Death Mode Regulation of HepG2 Cells

SUNG-CHUL LIM^{1,2*}, KESHAB RAJ PARAJULI^{2*} and SONG IY HAN^{2,3}

¹Department of Pathology, College of Medicine, Chosun University, Gwangju, Republic of Korea;

²Research Center for Resistant Cells, Chosun University, Gwangju, Republic of Korea;

³Division of Premedical Science, College of Medicine, Chosun University, Gwangju, Republic of Korea

Abstract. *Background/Aim:* We previously showed that oxaliplatin induces necrotic-like cell death in hepatocarcinomas, and combination with ursodexoycholic acid (UDCA) significantly shifts the necrotic-like death to apoptosis. Since cell death mode is crucial on inflammatory responses and chemotherapeutic efficacy, the mechanism underlying determination of cell death mode by UDCA was investigated in this study. *Materials and Methods:* Apoptosis or necrosis was determined by apoptotic body formation, caspase-8 activity, LDH release and PI inclusion. The involvement of lipid rafts and death receptors was examined by rafts fractionation, confocal microscopy and gene silencing assays. *Results:* UDCA combination enhanced recruitment of death receptors and adaptors into cholesterol-enriched lipid rafts, and induced a stronger raft clustering. Lipid raft disruption decreased the UDCA/oxaliplatin-mediated apoptosis and increased necrotic-like death. *Conclusion:* UDCA promotes lipid raft localization of multiple death receptors, thereby contributing to a shift of cell death mode from oxaliplatin-induced necrotic death to apoptosis in HepG2 cells.

Cancer cells respond to chemotherapy by undergoing apoptosis or necrosis. Cells that are dead by necrosis lose the integrity of the plasma membrane, leading to the dispersal of their cytoplasmic contents (*i.e.*, high mobility group box 1) into the extracellular space, ultimately resulting in inflammatory responses in the physiological environment (1-3).

*These Authors contributed equally to this study.

Correspondence to: Professor Song Iy Han, Division of Premedical Science, College of Medicine, Chosun University, Gwangju 61452, Republic of Korea. Tel: +82 622306194, e-mail: sihan@chosun.ac.kr

Key Words: Cell death mode, lipid rafts, apoptotic death, necrotic death.

Unlike necrosis, apoptotic cells are compacted into membrane-wrapped apoptotic bodies and are removed by phagocytes, so that the intracellular inflammation-inducing substances are not released to the outside and do not cause a serious inflammatory response. Acute inflammation by some microbes has been reported to contribute to treatment of bladder cancer, whereas certain types of chronic inflammation were shown to promote tumorigenesis and progression. Therefore, the cell death mode is closely related to inflammatory response and may affect the outcome of cancer treatment (4, 5).

Apoptosis is mainly controlled by two different signaling pathways: the cell surface death receptor-mediated extrinsic pathway involving caspase-8 activation and the mitochondria-associated intrinsic pathway inducing caspase-9 activation. Upon activation of the death receptor, a death-inducing signaling complex (DISC) containing the Fas-associated death domains (FADD) and the initiator caspase-8 is formed, resulting in activation of caspase-8 and subsequently downstream of caspase-3 (6-8). Several death receptors belonging to the tumor necrosis factor (TNF) receptor superfamily, including CD95/Fas and TNF-related apoptosis-inducing ligand receptors (TRAILR/DR), have been implicated in the induction of apoptotic cell death (9). Recently, several common points of apoptotic and necrotic pathways by TNFR have been found, and the regulation at this point can switch from apoptosis to necrosis and *vice versa* (10, 11).

The plasma membrane is a highly dynamic cellular structure through which various signaling events are actively regulated. Alterations in membrane events, such as membrane fluidity or lipid raft formation, appear to be closely associated with cellular susceptibility to apoptosis (12, 13). Furthermore, chemotherapeutic drugs have been shown to induce cell membrane fluidity and the formation of large lipid rafts (14-16). The lipid rafts are cholesterol-enriched and tightly ordered microdomains of the plasma membrane, and when they are connected to form larger rafts, they contribute to the amplification of the membrane

receptor-mediated signaling pathway (17). Therefore, the cell membrane appears to be an important structure for regulating various cell signaling pathways including cell death.

Previously, we observed that oxaliplatin, a platinum-based chemotherapeutic drug having anti-tumor efficacy in advanced cancers, induces mainly necrosis in hepatocarcinoma cells, whereas it mainly triggers apoptotic death in colon cancer cells (18). Ursodeoxycholic acid (UDCA), a hydrophilic bile acid, is widely used for the treatment of cholestatic liver diseases based on its cytoprotective and immunomodulatory activities (19, 20). It has also been shown to suppress carcinogenesis in several pre-malignant conditions in the liver and colon (21, 22). We observed that UDCA switches oxaliplatin-induced necrotic cell death to apoptotic death in HepG2 cells by enhancing caspase-8 activity (18). Recently, it was shown that UDCA is incorporated into the plasma membrane of hepatocytes in a similar way to cholesterol, and plays a role as a membrane stabilizer thereby protecting cells from oxidative stress. Though alteration of membrane events is one of crucial factors of cell death control, its effect on the cell death mode is still unknown. Herein, we showed that the events of lipid raft formation in cell membrane are related to cell death mode determination.

Materials and Methods

Cell culture and drug treatment. A human hepatocarcinoma HepG2 cell line was grown in RPMI 1640 medium (Invitrogen, Carlsbad, CA, USA) supplemented with 10% (v/v) fetal bovine serum (FBS; Invitrogen) and 1% penicillin-streptomycin (Welgene, Seoul, Republic of Korea) in a 37°C humidified incubator in an atmosphere of 5% CO₂. Drug treatment of cells was performed by adding 50-100 μM oxaliplatin (L-OHP; Boryung Pharmaceutical, Seoul, Republic of Korea) with or without 100 μM UDCA (ICN Biomedicals, Irvine, CA, USA). Unless specified otherwise, drugs were purchased from Calbiochem (San Diego, CA, USA).

Apoptotic measurement by Hoechst 33342 (HO)/propidium iodide (PI) double staining. Treated cells were incubated with a HO (Invitrogen, 1 μg/ml)/PI (5 μg/ml) mixture at 37°C for 15 min in the dark. Then, both floating and attached cells were collected. The pooled cell pellets were washed with ice-cold phosphate-buffered saline (PBS), fixed in 3.7% formaldehyde on ice, washed again with PBS, resuspended and a fraction of the suspension was centrifuged in a cytospinner. The slides were air dried, mounted and observed under a DM5000 fluorescence microscope (Leica, Jena, Germany), as described elsewhere (18). Morphological assessments of apoptosis and necrosis were performed; intact blue nuclei, condensed/fragmented blue nuclei, condensed/fragmented pink nuclei and intact pink nuclei were considered viable, early apoptotic, late apoptotic (secondary necrotic) and necrotic cells, respectively. A total of 500 cells from randomly chosen fields were counted, and the number of apoptotic cells was expressed as a percentage of the total number of cells counted.

Lactate dehydrogenase (LDH) release and 3-(4, 5-dimethylthiazol-2-yl)-2, 5-diphenyltetrazolium bromide (MTT) viability assay. LDH release was quantified using the LDH cytotoxicity assay kit II (BioVision, Mountain View, CA, USA) according to the manufacturer's protocol (18). The percentage of specific LDH release was calculated by the following formula:

$$\% \text{ cytotoxicity} = \frac{(\text{experimental LDH release}) - (\text{spontaneous LDH release by effector and target})}{(\text{maximum LDH release}) - (\text{spontaneous LDH release})} \times 100$$

For the MTT assay, cells were incubated with MTT solution (0.5 mg/ml) and solubilized using dimethylsulfoxide, and the solubilized formazan product was quantified at an absorbance of 595 nm as described elsewhere (18).

Immunoblotting. Equal amounts of protein were electrophoretically separated using 10~12% sodium dodecyl sulfate-polyacrylamide gel electrophoresis (SDS-PAGE) and transferred to a nitrocellulose membrane using a standard technique. Antibodies were used to probe for full-size caspase-8, cleaved caspase-3 (Cell Signaling Technology, Danvers, MA, USA), poly (ADP-ribose) polymerase (PARP), Fas, FADD, RIP1, caveolin-1 (Santa Cruz Biotechnology, Santa Cruz, CA, USA), DR4, and DR5 (ProSci, Poway, CA, USA). Anti-α-tubulin (BioGenex, San Ramon, CA) was used as a loading control. Signals were acquired using an Image Station 4000MM image analyzer (Kodak, Rochester, NY, USA).

Caspase-8 activity assay. Caspase-8 activity assay was carried out using a FADD-like IL-1β-converting enzyme (FLICE) colorimetric assay kit (BioVision, Milpitas, CA, USA), according to the manufacturer's protocol. Briefly, 200 μg of protein lysates in a 50-μl volume was mixed with a reaction buffer, mixed with IETD-pNA substrate, incubated for 90 min, and the absorbance at 405 nm measured. A fold increase in FLICE activity was determined by comparing the results of the treated samples with the level of the untreated control.

Real-time RT-PCR. Real-time PCR was performed with the Light Cycler 2.0 (Roche, Basel, Switzerland) using a Fast Start DNA Master SYBR Green I Kit (Roche). For verification of the correct amplification product, PCR products were analyzed on 2% agarose gel stained with ethidium bromide. The sequences of the primers were as follows: for β-actin; 5'-GACTATGACTTAGTTGCGTTA-3' and 5'-GCCTTCATACATCTCAAGTTG-3' for CD95/Fas; 5'-TGGCACGGAACACACCCTGAGG-3' and 5'-GAGGGTCCAGATGCCAGCATG-3', for TRAILR-1/DR4; 5'-ATGGCGCCAC CACCAGCTAGAG-3' and 5'-CCCGCCTCGTGGTTCAATCCTC-3', for TRAILR-2/DR5; 5'-GCCTCATGGACAATGAGATAA AGGTGGCT-3' and 5'-CCAAATCTCAAAGTACGCACAAAAC GG-3', for TRAILR-3/DcR1; 5'-AGGATCTCATAGATCAGAA CATACT-3' and 5'-ACACTGTGTCTCTGGTCA-3', for TRAILR-4/DcR2; 5'-CGGAGGAGACAGTGACC-3' and 5'-CCTGAGC AGATGCCTTTGA-3'. A melting curve analysis was performed to confirm production of a single product. Negative controls without a template were produced for each run. Data were analyzed using Light Cycler software version 4.0 (Roche).

RNA interference (RNAi). For the RNAi experiment, siRNA of TRAILR-1/DR4, 5'-CUGGAAAGUUAUCUACUU(dtdt)-3' (sense) and 5'-AAGUAGAUGAACUUUCCAG(dtdt)-3' (anti-sense),

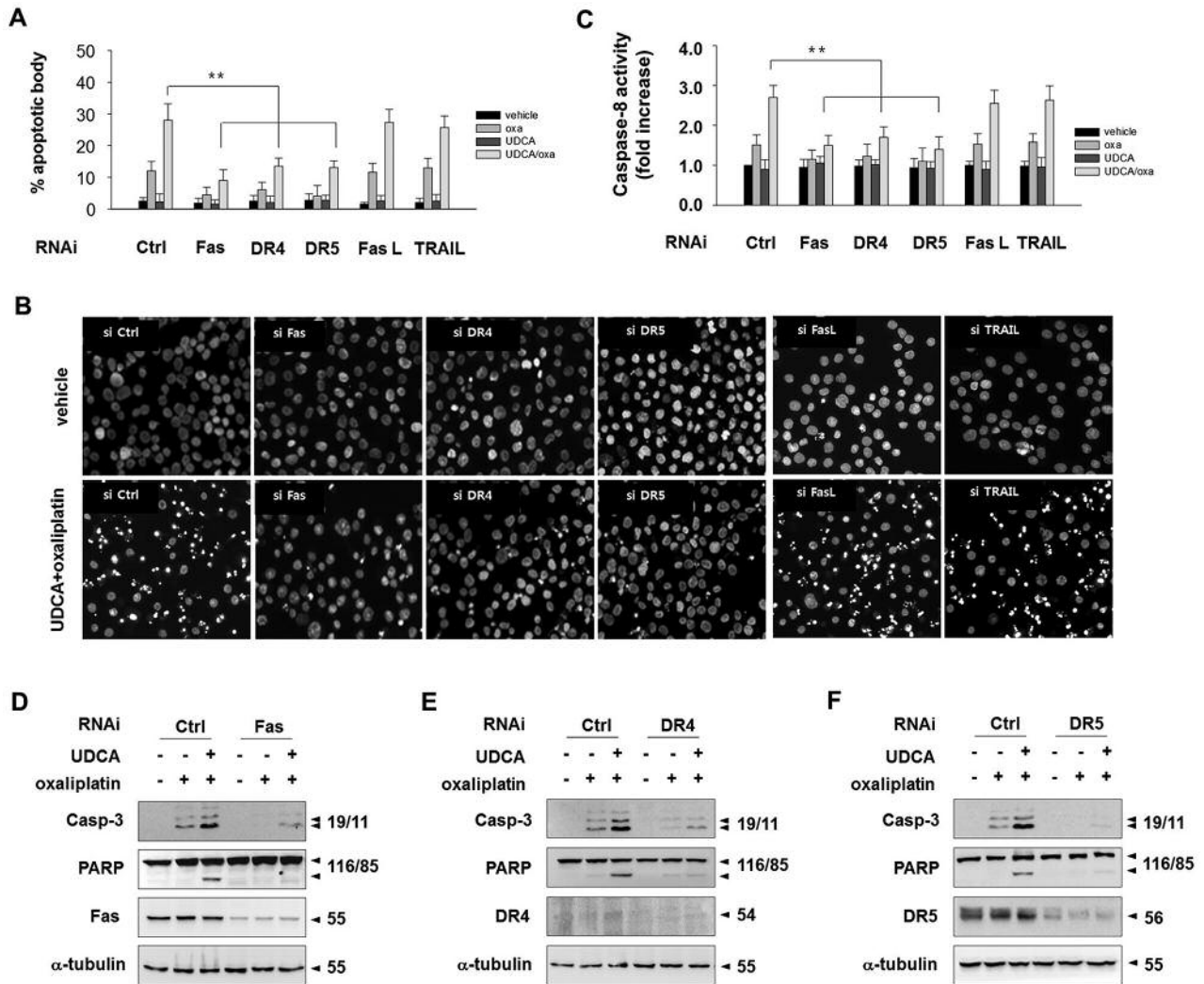


Figure 1. Multiple death receptors are involved in UDCA/oxaliplatin-induced apoptosis in HepG2 cells. (A-C) HepG2 cells transiently transfected with siRNA for CD95/Fas, TRAILR-1/DR4, TRAILR-2/DR5, Fas L, TRAIL, or scrambled RNA (si Ctrl) were exposed to vehicle, 50 μ M oxaliplatin or 100 μ M UDCA plus 50 μ M oxaliplatin for 24 h. Apoptotic bodies were visualized by Hoechst33342 staining and scored (A) or photographed (B) under a fluorescence microscope, or caspase-8 activity was measured using IETD-pNA substrate (C). $**p < 0.01$. (D-F) Cells transfected with scrambled siRNA and siRNA for CD95/Fas (D), TRAILR-1/DR4 (E), and TRAILR-2/DR5 (F) were treated with 50 μ M oxaliplatin or 100 μ M UDCA/50 μ M oxaliplatin for 24 h and analyzed by immunoblotting to detect cleaved caspase-3, PARP, CD95/Fas, TRAILR-1/DR4, and TRAILR-2/DR5. α -Tubulin was used as a loading control.

TRAILR-2/DR5, 5'-CAGACUUGGUGCCCUUUG(dtdt)-3' (sense) and 5'-UCAAGGGCACCAAGUCUG(dtdt)-3' (anti-sense), CD95/Fas, 5'-GAGAGUAUUACUAGAGCUU(dtdt)-3' (sense) and 5'-AAGCUCUAGUAAUACUCUC(dtdt)-3' (anti-sense), and TRAIL, 5'-CUCCUUGUAAAAGACUGUAG(dtdt)-3' (sense) and 5'-CUACAGUCUUUACAAGGAG(dtdt)-3' (anti-sense), and FasL, 5'-CUCAGACGUUUUUCGGCUU(dtdt)-3' (sense) and 5'-AAGCGAAAAACGUCUGAG(dtdt)-3' (anti-sense), 5'-control siRNA, 5'-CCUACGCCACCAAUUCGU(dtdt)-3' (sense) and 5'-ACGAAAUUGGUGGCGUAGG(dtdt)-3' (anti-sense) were purchased from Bioneer (Daejeon, Republic of Korea). Cells were cultured on 6-well cell culture plates (at a density of 2×10^5 cells per well) and

transfected with a mixture of 100 ng of siRNA and 4 μ l of INTERFERin™ reagent (Polyplus-Transfection, Illkirch, France). Cells were grown for 24 h prior to treatment.™

Lipid raft fractionation. Lipid rafts were isolated by sucrose density-gradient centrifugation. A total of 10^8 cells were lysed for 30 min in 1 ml of lysis buffer (1% Brij35 in HEPES buffer; 25 mM HEPES, 1 mM EDTA, and 150 mM NaCl, pH 6.5) supplemented with a protease inhibitor cocktail and then homogenized with a glass Dounce homogenizer. The homogenates were mixed with 1 ml of 80% sucrose in a HEPES buffer and placed at the bottom of a centrifuge tube. The samples were then overlaid with 6.5 ml of 30%

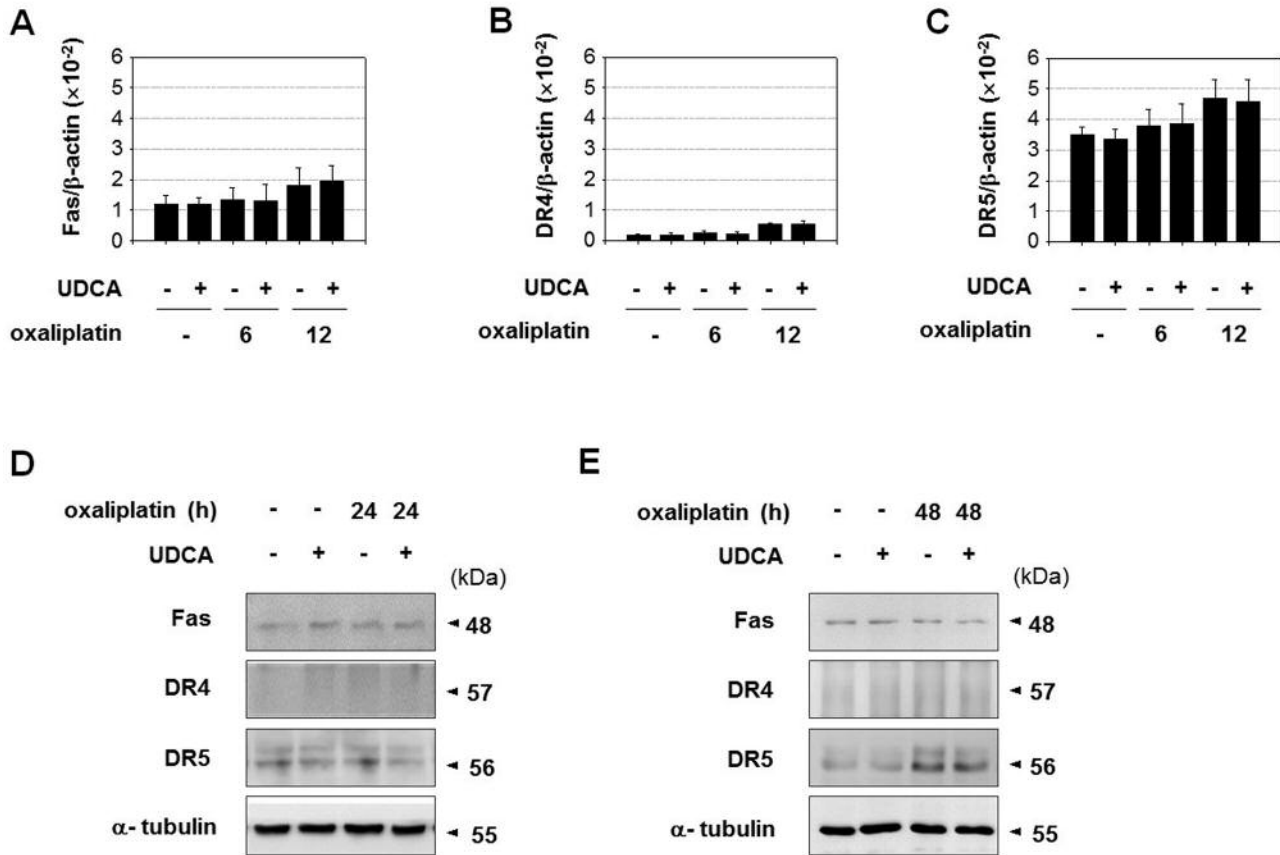


Figure 2. Expression of CD95/Fas, TRAILR-1/DR4, and TRAILR-2/DR5 was not altered in the presence of UDCA. HepG2 cells were exposed to 50 μ M oxaliplatin in the presence or absence of 100 μ M UDCA for the indicated times, and the mRNA levels of death receptor were analyzed by real-time PCR (A-C). Protein levels of CD95/Fas, TRAILR-1/DR4 and TRAILR-2/DR5 were analyzed by immunoblotting at 24 and 48 h after oxaliplatin treatment (D).

sucrose and 3 ml of 5% sucrose and centrifuged at $188,000 \times g$ for 18 h at 4°C. Fractions (1 ml) were collected from the bottom to the top of the gradient and precipitated, and the distribution of the various proteins was assessed by immunoblotting. The total protein in each fraction was determined using a Bio-Rad Protein Assay Kit, and total cholesterol was determined using a total cholesterol assay kit (Wako Diagnostics, Richmond, VI, USA).

Confocal microscopy. Cells grown on cover slips were treated, fixed with 1.5% paraformaldehyde for 10 min at -20°C, and then blocked with 5% bovine serum albumin/phosphate buffered saline for 1 h at room temperature. The cells were then incubated with anti-DR5 antibody and reacted with a rhodamine-conjugated secondary antibody, followed by further incubation with 10 μ g/ml of fluorescein isothiocyanate-labeled cholera toxin B (FITC-CTxB) and 1 μ g/ml of HO for 30 min. Cellular localization of both anti-DR5 and rafts was observed under a FV1000 laser-scanning confocal microscope at $\times 600$ magnification (Olympus). FITC and rhodamine were excited at 488 nm with an argon laser, and the evoked emission was filtered with a 515 nm (FITC) or 515-605 nm (rhodamine) band-pass filter. HO was excited at 405 nm with a diode laser, and emission was filtered at 400-450 nm.

Statistical analysis. Data are expressed as mean \pm S.E. of the averaged values obtained from each experiment. All data represent the results of at least 3 independent experiments. Statistical significance was determined by a Student's *t*-test and one-way ANOVA. A *p*-value of <0.05 was considered statistically significant.

Results

Multiple death receptors are involved in UDCA/oxaliplatin-induced apoptosis. Previously, we showed that 24-h exposure of 50 μ M oxaliplatin induces mainly necrosis ($32.8 \pm 4.7\%$) and, to a lesser extent, apoptosis ($11.2 \pm 5.4\%$) in HepG2 cells whereas the combination of UDCA with oxaliplatin shifts the cell death mode from necrosis to apoptosis by elevating the caspase-8 activity (23). In this study, we sought to understand the mechanism underlying cell death mode control by UDCA combination in oxaliplatin-induced cell death. Since caspase-8 is the main initiator protease activated by the extrinsic death receptor pathway, we first investigated whether this event is associated with activation of the death

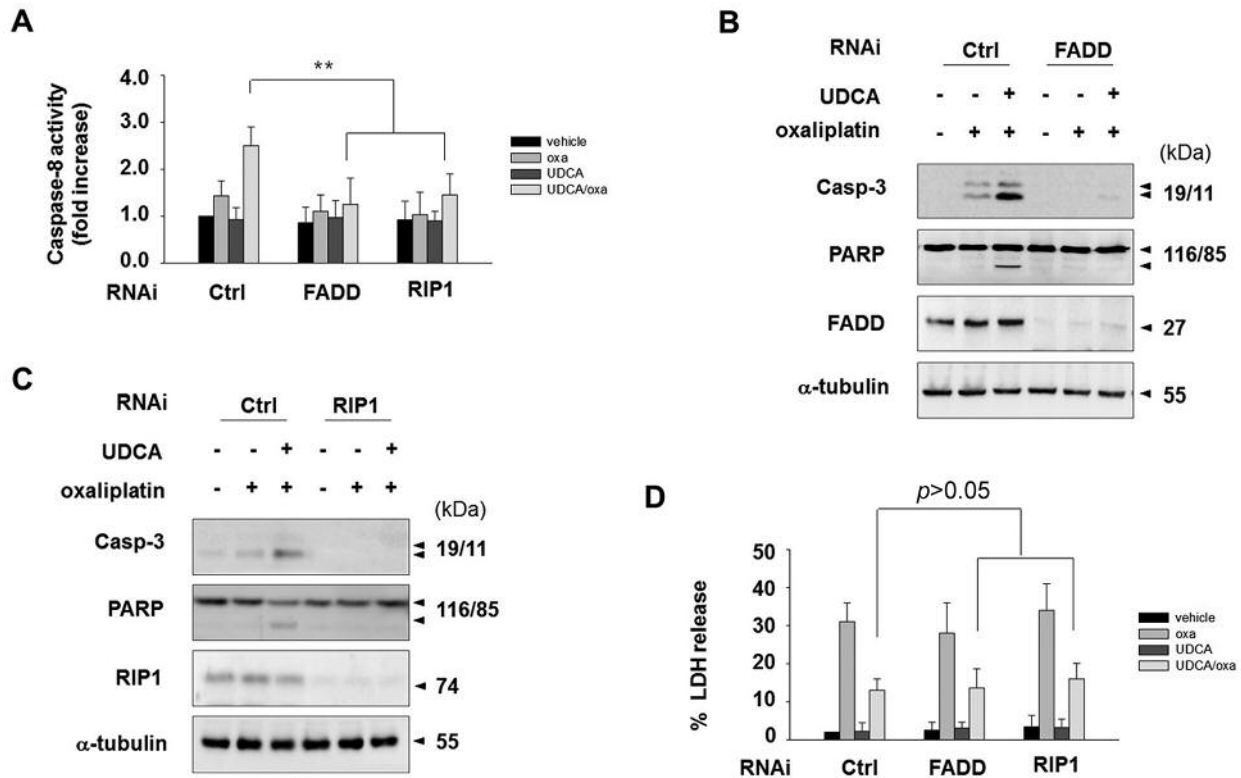


Figure 3. UDCA/oxaliplatin-induced apoptotic signals are transmitted through FADD and and RIP1. Cells transfected with scrambled siRNA, FADD siRNA and RIP1 siRNA were exposed to 50 μ M oxaliplatin or 100 μ M UDCA/50 μ M oxaliplatin for 24 h, and analyzed for caspase-8 activity assays (A), immunoblotting using antibodies against cleaved caspase-3 (p17/19), PARP, FADD, and α -tubulin (B), or LDH release assay (C) $**p < 0.01$.

receptor pathway. CD95/Fas, TRAILR-1/DR4, and TRAILR-2/DR5 are major death receptors that induce apoptosis in response to their ligands, FasL and TRAIL, in tumor cells. Thus, we investigated the possible involvement of death receptors and their ligands in UDCA/oxaliplatin-induced apoptosis using transient transfection of small interfering RNA (siRNA) specific for CD95/Fas, TRAILR-1/DR4, TRAILR-2/DR5, FasL, and TRAIL. Compared to the control RNA transfected cells (34.6 \pm 5.4%), transfection with CD95/Fas- (10.3 \pm 5.7%), TRAILR-1/DR4- (14.6 \pm 6.5%), or TRAILR-2/DR5- (14.8 \pm 3.1%) specific siRNA, but not FasL- (36.6 \pm 5.9%), or TRAIL (31.7 \pm 4.8%) siRNA, significantly prevented the apoptosis induced by UDCA/oxaliplatin, as demonstrated by the suppression of apoptotic body formation (Figure 1A and B) and caspase-8 activity assay (Figure 1C). Similar results were obtained in caspase-3 and PARP cleavages (Figure 1D-F). These results imply that UDCA-promoted oxaliplatin-induced apoptosis is executed by ligand-independent multiple death receptor pathways. However, UDCA combination did not affect the mRNA (Figure 2A-C) and protein levels of these death receptors (Figure 2D and E), indicating that the activation of multiple

death receptor pathway enhanced by UDCA combination may not be caused by an increase of death receptor expression. These results indicate that UDCA promotes activities of multiple death receptors not affecting expression of death receptors.

UDCA/oxaliplatin-induced apoptotic signal is transmitted through FADD and RIP1. As a downstream adaptor of death receptors, FADD is an essential factor for caspase-8 recruitment and apoptosis execution. The kinase receptor interacting protein 1 (RIP1) is another adaptor protein of death receptors, implicated in the control of apoptosis as well as necroptosis. To investigate whether the death mode regulation is related with a role of adaptor protein, we observed the effect of knockdown of RIP1 or FADD. When FADD or RIP1 expression was interfered by siRNA, UDCA/oxaliplatin-induced caspase-8 activation was prevented (Figure 3A), and cleavage of caspase-3 and PARP were also prevented (Figure 3B and C). However, LDH release was not significantly altered by interference of these adaptor proteins (Figure 3D). Thus, FADD and RIP1 may only transmit multiple death receptor-mediated apoptotic

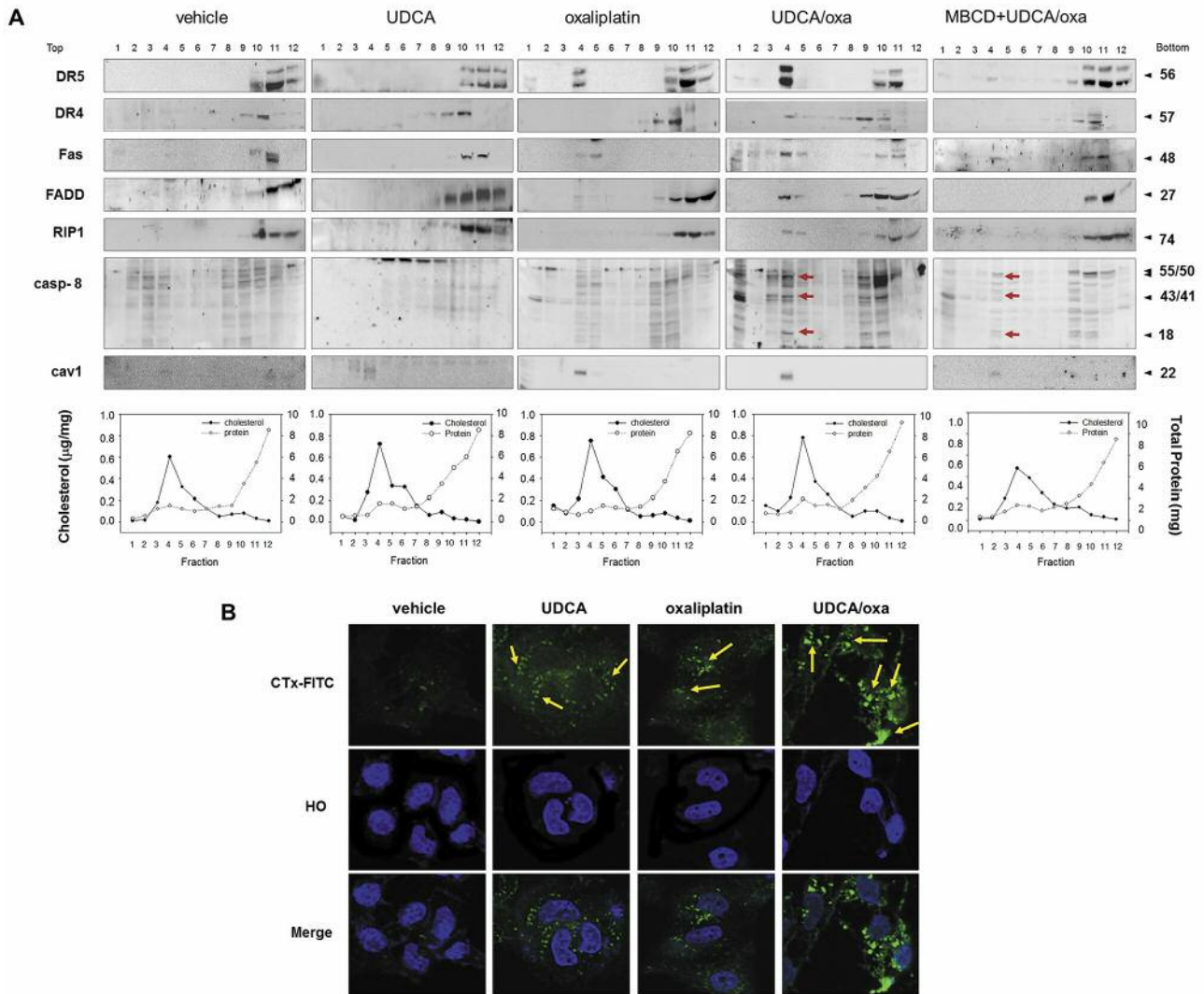


Figure 4. Oxaliplatin-triggered re-localization of DISC proteins into the raft fraction and lipid raft aggregation is facilitated by UDCA. (A) HepG2 cells were exposed to vehicle, 50 μ M oxaliplatin, 100 μ M UDCA/50 μ M oxaliplatin, or 1mM MBCD plus 100 μ M UDCA/50 μ M oxaliplatin, followed by lysis in a 1% Brij lysis buffer and fractionation by 5-40% sucrose density gradient centrifugation. Fractionated samples were analyzed for cholesterol and total protein content (lower) or were precipitated and subjected to immunoblotting to detect CD95/Fas, TRAILR-2/DR5, FADD, caspase-8, and caveolin-1 (upper). (B) HepG2 cells plated onto cover slips in 6 well-plates were treated with vehicle, 100 μ M UDCA, 50 μ M oxaliplatin, and 100 μ M UDCA plus 50 μ M oxaliplatin for 3 h. Treated cells were fixed with 1.5% paraformaldehyde, rinsed, and stained with CTx-FITC/Hoechst 33342, then mounted and observed by confocal microscopy.

signals to caspase-8 activation, but not be involved in the regulation of death mode in this system. Thus, adaptor proteins may not play a role in decision of cell death mode in this system.

UDCA enhances recruitment of DISC proteins into the lipid raft region. In apoptosis triggered by pro-apoptotic stimuli such as anti-cancer agents, death receptors are known to localize into lipid rafts for the activation of downstream death inducing signaling (24, 25). UDCA has a similar

structure with cholesterol, which contributes to the biophysical properties of the lipid rafts, and UDCA can be incorporated into the plasma membrane and affect membrane fluidity (26, 27). Herein, we examined whether a combined UDCA treatment enhances the localization of death receptors into lipid rafts. To this end, cells were lysed using 1% Brij following a conventional method and separated by discontinuous 5-40% sucrose density-gradient centrifugation. A total of 12 fractions, each 1 ml in volume, were collected from the bottom (Fraction 12) to top (Fraction 1) and

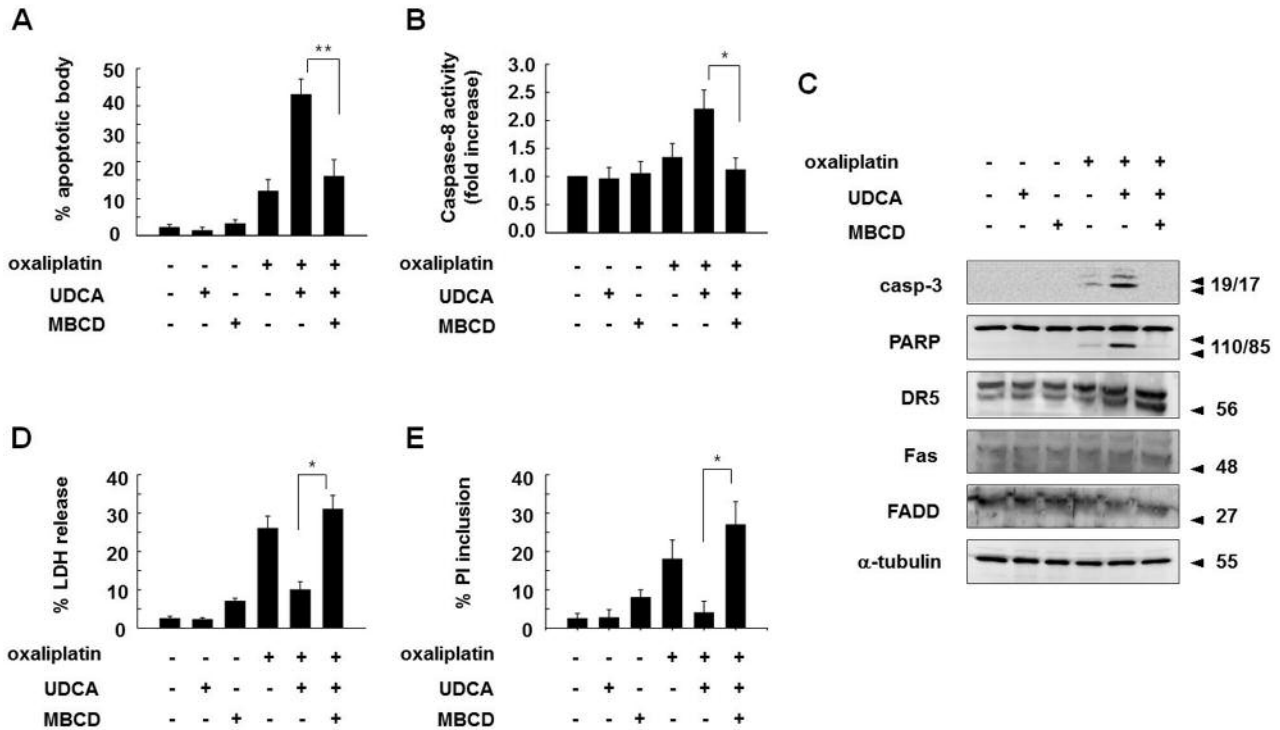


Figure 5. Methyl β -cyclodextrin (MBCD) reverts UDCA/oxaliplatin-induced apoptotic death into necrotic death. HepG2 cells were incubated with 50 μ M oxaliplatin for 24 h in the presence (+) or absence (-) of 100 μ M UDCA and/or 2.5 mM MBCD, after which cells were subjected to Hoechst 33342 staining to assess apoptotic body formation and caspase-8 activity (A and B), immunoblotting to detect active caspase-3, PARP, TRAILR-2/DR5, CD95/Fas, FADD, and α -tubulin (C), LDH release assay, and PI inclusion (D and E). * $p < 0.05$, ** $p < 0.01$.

analyzed biochemically for their cholesterol and protein content. In the control or UDCA-treated sample, CD95/Fas, TRAILR-1/DR4 and TRAILR-2/DR5 were only observed in bottom Fractions around 10-12. However, upon exposure to oxaliplatin, re-localization of death receptors was weakly observed in Fraction 4, which was characterized as a raft fraction based on its high cholesterol content and caveloin-1 localization, and combination with UDCA further increased these bands in Fraction 4. Likewise, FADD, RIP1 and caspase-8 were translocated into the raft fraction by oxaliplatin treatment and, more strongly, by UDCA combination with oxaliplatin (Figure 4A). Addition of a lipid raft disrupting agent, methyl β -cyclodextrin (MBCD), to UDCA/oxaliplatin blocked re-localization of DISC proteins into Fraction 4, confirming lipid raft-association of these factors. Next, we also performed immunofluorescence to investigate the ability of UDCA to induce raft formation. For this purpose, we visualized lipid rafts by staining cells with a raft marker, FITC-CTxB. As shown in Figure 4B, small raft structures were observed upon treatment with oxaliplatin or UDCA, and when UDCA was treated in combination with oxaliplatin, larger intense raft structures were observed. The collective data support the idea that co-treatment of UDCA

enhances oxaliplatin-triggered raft clustering and recruitment of DISC proteins into raft regions.

Lipid raft clustering is critical for UDCA-mediated switch of oxaliplatin-induced necrosis to apoptosis. We examined the possibility that lipid rafts act as an upstream regulator of cell death mode that leads to activation of pathways of multiple death receptors. Addition of a raft disrupting agent, MBCD, clearly suppressed UDCA/oxaliplatin-induced apoptosis, as shown in Hoechst 33342 staining and a caspase-8 activity assay (Figure 5A and B). Cleavages of caspase-3 and PARP were also blocked by MBCD, not affecting CD95/Fas and TRAILR-2/DR5, and FADD protein levels (Figure 5C). Moreover, co-treatment with MBCD and UDCA/oxaliplatin re-elevated the level of LDH release and propidium iodine (PI) inclusion, which are markers of membrane leakage (Figure 5D and E). The re-elevation of necrotic features indicated that MBCD switched the cell death pattern back to necrotic-like death. Hence, cell death fate induced by oxaliplatin seems to be closely associated with lipid raft formation and UDCA is likely to be involved in the stimulation of raft formation when combined with oxaliplatin.

Discussion

Since raft formation is a critical event to control death receptor signaling and apoptosis, we examined the role of UDCA on lipid rafts and investigated the possible involvement of lipid rafts in UDCA-mediated apoptotic switch (18). Interestingly, using raft isolation assays, we observed that UDCA enhanced oxaliplatin-induced recruitment of DISC proteins into high cholesterol-distributed raft fractions, which was prevented by MBCD. More importantly, the UDCA-potentiated necrosis-to-apoptosis switch appeared to be controlled by lipid rafts. MBCD prevented both raft formation and apoptosis and restored necrotic release of LDH, indicating a critical role for lipid rafts in the UDCA-mediated switch of cell death mode. Raft disruption by MBCD may not only prevent apoptosis by inhibiting activation of death receptors, but also induce necrosis by influencing the activities of various necrosis-related signaling molecules.

Lipid rafts are cholesterol-enriched, tightly-ordered microdomains of the plasma membrane acting as signaling platforms, and larger rafts contribute to signal amplification (17). In this study, UDCA appears to contribute to the formation of larger or denser raft platforms regarding the facts that UDCA combination induces larger CTx-stained raft structures and stronger distribution of DISC proteins in the raft-isolated fractions. It is noteworthy that this apoptotic pathway was regulated by multiple death receptors, not by one specific death receptor, and knockdown of any of the three death receptors apparently reduced apoptosis. This result implies that cooperative action of multiple death receptors is required for efficient apoptosis induction, which may be supported by lipid raft aggregation.

Cisplatin and oxaliplatin, platinum-based chemotherapeutic drugs, are DNA-alkylating agents that interact with cellular proteins, particularly HMG domain proteins, to induce apoptosis in proliferating cancer cells (28, 29). In addition, these platinum drugs induce changes in the fluidity of the cellular membrane and formation of large lipid rafts (14, 15, 30, 31), and lipid raft aggregation is a critical step in platinum drug-induced apoptosis; CD95/Fas localization into lipid rafts is required for cisplatin-induced apoptosis, and oxaliplatin promotes TRAIL-induced apoptosis by inducing TRAILR-1/DR4 and TRAILR-2/DR5 redistribution into lipid rafts (15, 25). We also observed that oxaliplatin induced raft formation and eventually apoptosis in SNU1, SNU601, SNUC5, HCT116, and HT29 cells (data not shown). However, in HepG2 cells, raft formation was not efficiently induced upon oxaliplatin exposure, and the raft formation could be fully activated by the presence of UDCA. Thus, the oxaliplatin-induced raft-forming ability seems to be cell type-specific, although the mechanism underlying this phenomenon remains to be clarified. Herein, we questioned whether breakdown of

lipid rafts will switch apoptosis to necrosis in the cell lines where apoptosis was induced by oxaliplatin. In our preliminary study, oxaliplatin treatment under prevention of lipid raft formation by MBCD resulted in two different cell fates: oxaliplatin-induced apoptosis was switched to necrosis in SNU1, SNU601, and SNUC5 cells, whereas oxaliplatin-induced apoptosis was prevented but not switched to necrosis in HCT116 and HT29 cells (data not shown). Hence, the role of raft formation in the cell fate may vary depending on cell type, determining cell death or survival in some cases and apoptosis or necrosis in others. The differential response may be due to a distinct cellular program linked to a crucial cell death checkpoint.

UDCA has a similar structure to cholesterol, which contributes to the biophysical properties of the lipid membrane, and UDCA is known to act as a membrane stabilizer (26, 32). Hence, we asked if cell membrane stability is associated with raft formation and apoptotic switch upon exposure to oxaliplatin. When oxaliplatin was treated in combination with various membrane-stabilizing agents such as cholesterol, catechin, and vitamin E, oxaliplatin-induced necrosis was attenuated, and membrane fluidizers such as dimethylsulfoxide, Tween 20, and phosphatidylcholine increased oxaliplatin-induced necrosis (data not shown). Therefore, membrane stability seemed to be related with the execution of necrosis. However, combining membrane stabilizers with oxaliplatin showed differential effect on raft aggregation and apoptotic body formation. Cholesterol and catechin, but not vitamin E slightly increased oxaliplatin-induced raft formation and apoptotic body formation. This result supports the view that membrane stability is possibly linked with the suppression of necrosis, but not completely matched to the raft forming ability of UDCA. Thus, UDCA may possess some additional feature other than a membrane-stabilizing activity. Bile acids have been reported to trigger membrane cholesterol spikes and membrane perturbations in a hydrophobicity-dependent manner (33, 34). Hydrophobic bile acids such as deoxycholic acid (DCA) or chenodeoxycholic acid (CDCA) share a cholesterol backbone with UDCA but have much more cytotoxic effects on cells (35). Considering the 'cholesterol spike' that consists of high content of cholesterol, sphingolipids, and caveolin-1, this structure seems to be similar with lipid rafts. We also observed that DCA induced strong raft structures in various cells including HepG2 cells (data not shown). In general, the effect of hydrophobic bile acids is detrimental because excess hydrophobicity causes massive nonspecific cell membrane damage not only inducing the formation of rafts, as shown in the example of detergents. UDCA, on the other hand, has a much milder effect on cell membranes and instead protects cells from various cytotoxic stimuli including more hydrophobic bile acid, ethanol, and Fas ligands (36-38). However, UDCA can

trigger apoptosis in certain cases. UDCA induces raft-dependent apoptosis in stomach cancer cells and enhances apoptosis in combination with anti-cancer drugs, both presently and in previous studies (18, 39). Therefore, UDCA seems to retain the potential activity of raft induction, which may sensitize cells toward apoptosis depending on cellular environment. This may provide an explanation for why UDCA-potentiated apoptosis is induced only in a limited fashion and is observed in specific cases, and this concept could be expanded to the role of lipid rafts in cancer treatment.

Conflicts of Interest

The Authors declare no conflicts of interest.

Authors' Contributions

SIH designed and wrote the article. KRP performed the experiments and analyzed the data. SL analyzed the data and edited the manuscript.

Acknowledgements

This work was supported by a research Fund from Chosun University, 2017. The Authors thank Ms. Jeong Eun Choi for her excellent technical assistance.

References

- 1 Rock KL and Kono H: The inflammatory response to cell death. *Annu Rev Pathol* 3: 99-126, 2008. PMID: 18039143. DOI: 10.1146/annurev.pathmechdis.3.121806.151456
- 2 Vanden Berghe T, Kalai M, Denecker G, Meeus A, Saelens X and Vandennebeele P: Necrosis is associated with il-6 production but apoptosis is not. *Cell Signal* 18(3): 328-335, 2006. PMID: 16023831. DOI: 10.1016/j.cellsig.2005.05.003
- 3 Buja LM, Eigenbrodt ML and Eigenbrodt EH: Apoptosis and necrosis. Basic types and mechanisms of cell death. *Arch Pathol Lab Med* 117(12): 1208-1214, 1993. PMID: 8250690.
- 4 Demirag F, Unsal E, Yilmaz A and Caglar A: Prognostic significance of vascular endothelial growth factor, tumor necrosis, and mitotic activity index in malignant pleural mesothelioma. *Chest* 128(5): 3382-3387, 2005. PMID: 16304288. DOI: 10.1378/chest.128.5.3382
- 5 Vakkila J and Lotze MT: Inflammation and necrosis promote tumour growth. *Nat Rev Immunol* 4(8): 641-648, 2004. PMID: 15286730. DOI: 10.1038/nri1415
- 6 Krammer PH: Cd95's deadly mission in the immune system. *Nature* 407(6805): 789-795, 2000. PMID: 11048730. DOI: 10.1038/35037728
- 7 Sprick MR, Weigand MA, Rieser E, Rauch CT, Juo P, Blenis J, Krammer PH and Walczak H: Fadd/mort1 and caspase-8 are recruited to trail receptors 1 and 2 and are essential for apoptosis mediated by trail receptor 2. *Immunity* 12(6): 599-609, 2000. PMID: 10894160. DOI: 10.1016/s1074-7613(00)80211-3
- 8 Schulze-Osthoff K, Ferrari D, Los M, Wesselborg S and Peter ME: Apoptosis signaling by death receptors. *Eur J Biochem* 254(3): 439-459, 1998. PMID: 9688254. DOI: 10.1046/j.1432-1327.1998.2540439.x
- 9 Gaur U and Aggarwal BB: Regulation of proliferation, survival and apoptosis by members of the tnfr superfamily. *Biochem Pharmacol* 66(8): 1403-1408, 2003. PMID: 14555214. DOI: 10.1016/s0006-2952(03)00490-8
- 10 Vanden Berghe T, Kalai M, van Loo G, Declercq W and Vandennebeele P: Disruption of hsp90 function reverts tumor necrosis factor-induced necrosis to apoptosis. *J Biol Chem* 278(8): 5622-5629, 2003. PMID: 12441346. DOI: 10.1074/jbc.M208925200
- 11 Lemasters JJ: V. Necrapoptosis and the mitochondrial permeability transition: Shared pathways to necrosis and apoptosis. *Am J Physiol* 276(1 Pt 1): G1-6, 1999. PMID: 9886971. DOI: 10.1152/ajpgi.1999.276.1.G1
- 12 Becker KA, Gellhaus A, Winterhager E and Gulbins E: Ceramide-enriched membrane domains in infectious biology and development. *Subcell Biochem* 49: 523-538, 2008. PMID: 18751925. DOI: 10.1007/978-1-4020-8831-5_20
- 13 Bollinger CR, Teichgraber V and Gulbins E: Ceramide-enriched membrane domains. *Biochim Biophys Acta* 1746(3): 284-294, 2005. PMID: 16226325. DOI: 10.1016/j.bbamcr.2005.09.001
- 14 Dimanche-Boitrel MT, Meurette O, Rebillard A and Lacour S: Role of early plasma membrane events in chemotherapy-induced cell death. *Drug Resist Updat* 8(1-2): 5-14, 2005. PMID: 15939338. DOI: 10.1016/j.drug.2005.02.003
- 15 Lacour S, Hammann A, Grazide S, Lagadic-Gossmann D, Athias A, Sergeant O, Laurent G, Gambert P, Solary E and Dimanche-Boitrel MT: Cisplatin-induced cd95 redistribution into membrane lipid rafts of ht29 human colon cancer cells. *Cancer Res* 64(10): 3593-3598, 2004. PMID: 15150117. DOI: 10.1158/0008-5472.CAN-03-2787
- 16 Rebillard A, Tekpli X, Meurette O, Sergeant O, LeMoigne-Muller G, Vernhet L, Gorria M, Chevanne M, Christmann M, Kaina B, Counillon L, Gulbins E, Lagadic-Gossmann D and Dimanche-Boitrel MT: Cisplatin-induced apoptosis involves membrane fluidification via inhibition of nhe1 in human colon cancer cells. *Cancer Res* 67(16): 7865-7874, 2007. PMID: 17699793. DOI: 10.1158/0008-5472.CAN-07-0353
- 17 Simons K and Toomre D: Lipid rafts and signal transduction. *Nat Rev Mol Cell Biol* 1(1): 31-39, 2000. PMID: 11413487. DOI: 10.1038/35036052
- 18 Kim CH, Han SI, Lee SY, Youk HS, Moon JY, Duong HQ, Park MJ, Joo YM, Park HG, Kim YJ, Yoo MA, Lim SC and Kang HS: Protein kinase c-erk1/2 signal pathway switches glucose depletion-induced necrosis to apoptosis by regulating superoxide dismutases and suppressing reactive oxygen species production in a549 lung cancer cells. *J Cell Physiol* 211(2): 371-385, 2007. PMID: 17309078. DOI: 10.1002/jcp.20941
- 19 Marziani M, Francis H, Benedetti A, Ueno Y, Fava G, Venter J, Reichenbach R, Mancino MG, Summers R, Alpini G and Glaser S: Ca²⁺-dependent cytoprotective effects of ursodeoxycholic and tauroursodeoxycholic acid on the biliary epithelium in a rat model of cholestasis and loss of bile ducts. *Am J Pathol* 168(2): 398-409, 2006. PMID: 16436655. DOI: 10.2353/ajpath.2006.050126
- 20 Angulo P: Use of ursodeoxycholic acid in patients with liver disease. *Curr Gastroenterol Rep* 4(1): 37-44, 2002. PMID: 11825540. DOI: 10.1007/s11894-002-0036-9

- 21 Loddenkemper C, Keller S, Hanski ML, Cao M, Jahreis G, Stein H, Zeitz M and Hanski C: Prevention of colitis-associated carcinogenesis in a mouse model by diet supplementation with ursodeoxycholic acid. *Int J Cancer* 118(11): 2750-2757, 2006. PMID: 16385573. DOI: 10.1002/ijc.21729
- 22 Oyama K, Shiota G, Ito H, Murawaki Y and Kawasaki H: Reduction of hepatocarcinogenesis by ursodeoxycholic acid in rats. *Carcinogenesis* 23(5): 885-892, 2002. PMID: 12016164. DOI: 10.1093/carcin/23.5.885
- 23 Berndtsson M, Hagg M, Panaretakis T, Havelka AM, Shoshan MC and Linder S: Acute apoptosis by cisplatin requires induction of reactive oxygen species but is not associated with damage to nuclear DNA. *Int J Cancer* 120(1): 175-180, 2007. PMID: 17044026. DOI: 10.1002/ijc.22132
- 24 Reis-Sobreiro M, Gajate C and Mollinedo F: Involvement of mitochondria and recruitment of fas/cd95 signaling in lipid rafts in resveratrol-mediated antimyeloma and antileukemia actions. *Oncogene* 28(36): 3221-3234, 2009. PMID: 19561642. DOI: 10.1038/onc.2009.183
- 25 Liu H, Jiang CC, Lavis CJ, Croft A, Dong L, Tseng HY, Yang F, Tay KH, Hersey P and Zhang XD: 2-deoxy-d-glucose enhances trail-induced apoptosis in human melanoma cells through xbp-1-mediated up-regulation of trail-r2. *Mol Cancer* 8: 122, 2009. PMID: 20003459. DOI: 10.1186/1476-4598-8-122
- 26 Guldutuna S, Deisinger B, Weiss A, Freisleben HJ, Zimmer G, Sipos P and Leuschner U: Ursodeoxycholate stabilizes phospholipid-rich membranes and mimics the effect of cholesterol: Investigations on large unilamellar vesicles. *Biochim Biophys Acta* 1326(2): 265-274, 1997. PMID: 9218557. DOI: 10.1016/s0005-2736(97)00030-8
- 27 Guldutuna S, Zimmer G, Imhof M, Bhatti S, You T and Leuschner U: Molecular aspects of membrane stabilization by ursodeoxycholate. *Gastroenterology* 104(6): 1736-1744, 1993. PMID: 8388838. DOI: 10.1016/0016-5085(93)90653-t
- 28 Kasparkova J, Farrell N and Brabec V: Sequence specificity, conformation, and recognition by hmg1 protein of major DNA interstrand cross-links of antitumor dinuclear platinum complexes. *J Biol Chem* 275(21): 15789-15798, 2000. PMID: 10747955. DOI: 10.1074/jbc.M000777200
- 29 Huang JC, Zamble DB, Reardon JT, Lippard SJ and Sancar A: Hmg-domain proteins specifically inhibit the repair of the major DNA adduct of the anticancer drug cisplatin by human excision nuclease. *Proc Natl Acad Sci USA* 91(22): 10394-10398, 1994. PMID: 7937961. DOI: 10.1073/pnas.91.22.10394
- 30 Segui B and Legembre P: Redistribution of cd95 into the lipid rafts to treat cancer cells? *Recent Pat Anticancer Drug Discov* 5(1): 22-28, 2010. PMID: 7937961. DOI: 10.1073/pnas.91.22.10394
- 31 Vondalova Blanarova O, Jelinkova I, Szoor A, Skender B, Soucek K, Horvath V, Vaculova A, Andera L, Sova P, Szollosi J, Hofmanova J, Vereb G and Kozubik A: Cisplatin and a potent platinum(iv) complex-mediated enhancement of trail-induced cancer cells killing is associated with modulation of upstream events in the extrinsic apoptotic pathway. *Carcinogenesis* 32(1): 42-51, 2011. PMID: 21037225. DOI: 10.1093/carcin/bgq220
- 32 Oliva L, Beauge F, Choquart D, Montet AM, Guitaoui M and Montet JC: Ursodeoxycholate alleviates alcoholic fatty liver damage in rats. *Alcohol Clin Exp Res* 22(7): 1538-1543, 1998. PMID: 9802540.
- 33 Jean-Louis S, Akare S, Ali MA, Mash EA Jr., Meuillet E and Martinez JD: Deoxycholic acid induces intracellular signaling through membrane perturbations. *J Biol Chem* 281(21): 14948-14960, 2006. PMID: 16547009. DOI: 10.1074/jbc.M506710200
- 34 Akare S and Martinez JD: Bile acid induces hydrophobicity-dependent membrane alterations. *Biochim Biophys Acta* 1735(1): 59-67, 2005. PMID: 15951237. DOI: 10.1016/j.bbali.2005.04.006
- 35 Sagawa H, Tazuma S and Kajiyama G: Protection against hydrophobic bile salt-induced cell membrane damage by liposomes and hydrophilic bile salts. *Am J Physiol* 264(5 Pt 1): G835-839, 1993. PMID: 8498510. DOI: 10.1152/ajpgi.1993.264.5.G835
- 36 Henzel K, Thorborg C, Hofmann M, Zimmer G and Leuschner U: Toxicity of ethanol and acetaldehyde in hepatocytes treated with ursodeoxycholic or tauroursodeoxycholic acid. *Biochim Biophys Acta* 1644(1): 37-45, 2004. PMID: 14741743. DOI: 10.1016/j.bbamcr.2003.10.017
- 37 Azzaroli F, Mehal W, Soroka CJ, Wang L, Lee J, Crispe N and Boyer JL: Ursodeoxycholic acid diminishes fas-ligand-induced apoptosis in mouse hepatocytes. *Hepatology* 36(1): 49-54, 2002. PMID: 12085348. DOI: 10.1053/jhep.2002.34511
- 38 Neuman MG, Cameron RG, Shear NH, Bellentani S and Tiribelli C: Effect of tauroursodeoxycholic and ursodeoxycholic acid on ethanol-induced cell injuries in the human hep g2 cell line. *Gastroenterology* 109(2): 555-563, 1995. PMID: 7615206. DOI: 10.1016/0016-5085(95)90345-3
- 39 Ikegami T, Matsuzaki Y, Al Rashid M, Ceryak S, Zhang Y and Bouscarel B: Enhancement of DNA topoisomerase i inhibitor-induced apoptosis by ursodeoxycholic acid. *Mol Cancer Ther* 5(1): 68-79, 2006. PMID: 16432164. DOI: 10.1158/1535-7163.MCT-05-0107

Received March 3, 2020

Revised March 13, 2020

Accepted March 16, 2020